

Cerebral Near-Infrared Spectroscopy Correlates to Vital Parameters During Cardiopulmonary Bypass Surgery in Children

Jan Menke · Gerhard Möller

Received: 4 April 2013 / Accepted: 19 June 2013 / Published online: 13 July 2013
© Springer Science+Business Media New York 2013

Abstract Near-infrared spectroscopy (NIRS) can monitor changes in cerebral regional oxygen saturation (rSO₂) and tissue hemoglobin content (HbT). The relation between cerebral NIRS readings and vital parameters has not been analyzed before at a fine temporal scale. This study analyzed this relation during cardiopulmonary bypass (CPB) surgery in 10 children (0–9 years, 1,770 min of data records) by using a novel random-coefficient model. The analysis indicated that a small number of patients is sufficient for obtaining significant results with this model. Changes of vital parameters explained 84.7 % of rSO₂ changes and 90.7 % of HbT changes. Cerebral rSO₂ correlated positively with perfusion pressure and inversely with body temperature ($P < 0.05$). Cerebral HbT correlated positively with perfusion pressure, central venous pressure, and temperature and inversely with arterial oxygen saturation ($P < 0.05$). During hypothermic circulatory arrest, the half-life of the exponential rSO₂ decay correlated to the rSO₂ reserve ($P = 0.016$). In conclusion, NIRS readings of cerebral hemoglobin content and tissue oxygen saturation correlate well to vital parameters during CPB surgery in children. NIRS may therefore become a monitoring device for the neuroprotective optimization of those vital parameters.

Keywords Cardiopulmonary bypass · Child · Congenital heart defects · Brain · Oxygen metabolism · Near-infrared spectroscopy

Abbreviations

CPB Cardiopulmonary bypass
HbT Cerebral tissue hemoglobin content
NIRS Near infrared spectroscopy
rSO₂ Cerebral regional oxygen saturation

Introduction

Neurological sequels are still observed in some children after cardiopulmonary bypass (CPB) surgery. Among their multifactorial causes may be periods of low cerebral oxygenation that are clinically not obvious from standard monitoring technology [14]. Near-infrared spectroscopy (NIRS) is being studied as novel monitor of cerebral oxygenation [11, 14]. In principle, NIRS measures the content of oxygenated (HbO₂) and deoxygenated (HbD) hemoglobin within the vasculature underneath its sensor, which allows monitoring of tissue hemoglobin content (HbT = HbO₂ + HbD) and regional oxygen saturation (rSO₂ = HbO₂/HbT) [11]. Approximately 15–25 % of the cerebral vasculature is arterial, and 75–85 % is venous [26]. cerebral regional oxygen saturation (rSO₂) is therefore weighted toward its venous component, thus providing information about the cerebral oxygen extraction. Current NIRS monitors are best suitable for semiquantitative measurements because their readings may deviate from true absolute values due to estimation of optical pathlength, unknown offsets, and other causes.

Among children undergoing reparative heart surgery, a current study found that perioperative periods of diminished

Electronic supplementary material The online version of this article (doi:10.1007/s00246-013-0754-9) contains supplementary material, which is available to authorized users.

J. Menke (✉) · G. Möller
Department of Pediatrics, University Hospital Goettingen,
Robert-Koch-Strasse 40, 37075 Goettingen, Germany
e-mail: menke-j@t-online.de

cerebral oxygenation, as indicated by NIRS-based rSO_2 , are associated with neurodevelopmental abnormalities at 1-year follow-up [14]. Preventing such hypoxemic periods requires knowledge about their causative factors. Some NIRS studies have correlated cerebral rSO_2 to procedural landmarks during CPB, such as hypothermic circulatory arrest or rewarming [10, 21]. However, the relation between NIRS readings and vital parameters during pediatric CPB has generally not been analyzed at a fine temporal scale. A problem in doing so is that the optical pathlength, the influence of vital parameters, and unknown factors may vary interindividually. Such differences can be considered by a random-coefficient model that extends the well-known multiple regression analysis by random effects for the slopes and the intercept [15].

This study aimed at analyzing the relation of cerebral NIRS readings to vital parameters during CPB surgery in children at a minute scale by using a novel random-coefficient model.

Materials and Methods

Patients and CPB

Ten consecutive children scheduled for CPB surgery were prospectively included after obtaining informed parental consent. The study had been approved by the university hospital's Ethics Committee on human research. The CPB circuit used a membrane oxygenator and a nonpulsatile roller pump (Stöckert, Munich, Germany) with a standard flow of approximately 120 ml kg min. To achieve isovolemic hemodilution, the CPB circuit was primed with crystalloid, human albumin, and mostly some erythrocyte concentrate. In cases with hypothermic CPB, the hypothermia was achieved by core and blood cooling, and alpha-stat blood gas management was applied. General anesthesia was performed with intravenous fentanyl and midazolam and with inhaled isoflurane or sevoflurane.

Recording of Vital Parameters

During CBP surgery, rectal temperature (T_{rectal}), intravascular mean arterial pressure (MAP), and intravascular central venous pressure (CVP) from the patient's routine monitoring were manually recorded every minute. Central perfusion pressure (CPP) was determined as $CPP = MAP - CVP$. Every minute, arterial oxygen saturation (SaO_2) was recorded from the pulse oximetry monitoring (Radiometer, Copenhagen, Denmark) while the heart was beating, and during bypass circulation the SaO_2 was read from the blood oxygenator. Arterial blood gas measurements (pCO_2 , pH, and base excess; L2000, Eschweiler, Germany) were

determined at 37 °C with additional hematocrit values (Hct) at intervals of approximately 5–20 min. These measurements were linearly interpolated to minute intervals. For comparison, blood gas values with correction to the body temperature were evaluated [4].

NIRS Monitoring

Regional cerebral rSO_2 and HbT at the patient's forehead was measured by an NIRS monitor (Critikon Cerebral RedOx Monitor 2020; Johnson & Johnson Medical, UK). This spatially resolved NIRS monitor emits continuous-wave NIR laser light at four different wavelengths (776.5, 819.0, 871.4, and 908.7 nm) into the tissue underneath the NIRS sensor [27]. Within the cerebral tissue, the emitted NIR light is scattered and partially absorbed [27]. Due to scattering, the effective pathlength of the 776.5 nm photons is approximately five times longer than the direct emitter-detector distance, which is considered by a differential pathlength factor [25]. At longer wavelengths, scattering and, subsequently, the effective photon pathlength decreases, which is considered by wavelength-dependent scattering factors [25, 27]. The attenuated NIR intensities at the four different wavelengths are measured by two optodes that are spaced 13 and 45 mm apart from the emitter. This dual-optode construction accounts for potential changes in light-coupling at the NIRS emitter. In addition, a NIR-light emitting diode is placed equidistant between both optodes, and its attenuated light is measured by the optodes. This compensates for potential changes in light-coupling at the optodes, thus making the NIRS monitoring more robust. The principle of operation and the implemented algorithm to convert the measured light attenuations into estimates of oxygenated hemoglobin (HbO_2) and deoxygenated hemoglobin (HbD) concentrations have been described elsewhere [27]. Estimates of HbT ($HbT = HbO_2 + HbD$) and rSO_2 ($rSO_2 = HbO_2/HbT$) were calculated and displayed by the NIRS monitor. HbO_2 , HbD , and their sum HbT are hemoglobin concentrations ($\mu\text{mol/L}$), whereas rSO_2 is an oxygen saturation parameter (% units). By way of RS232 interface the readings of the NIRS monitor were electronically stored at 1-second intervals by an attached computer, and were then averaged to 1 dataset/min.

Random-Coefficient Analysis

Random-effects models are well-introduced in the literature; for instance they are used for bivariate meta-analysis and meta-regression of sensitivity and specificity [16, 17, 20]. In this study, data were analyzed by a hierarchical multivariate random-coefficient model [15]. In principle, this is a multiple linear regression analysis where the offset and the covariates' slopes may deviate individually from

the mean offset and the mean slopes, thus representing true but unknown interindividual differences. In the hierarchical modeling, these differences are assumed to be normally distributed among the patients. Such random-coefficient analysis was applied for the NIRS parameters, rSO₂ and HbT, as dependent variables. In each analysis, the seven vital parameters (i.e., CPP, CVP, T_{rectal}, SaO₂, Hct, pCO₂, and pH) were entered as the independent covariates. All parameters were individually centered by subtracting their mean. The NIRS parameter HbT and the blood pressure parameter CPP were expressed as a percentage deviation from their individual baseline. That baseline was obtained from the time period between –20 and –10 min before starting CPB. Per patient, any covariate was entered into the model only if it showed sufficient variation (Table 1); otherwise an according slope (e.g., ΔrSO₂ per ΔT_{rectal}) cannot be determined. The covariates were tested for collinearity that might affect the numerical stability of the statistical results. Relevant collinearity was assumed if the according variance inflation factor (VIF) exceeded ten [3]. The contribution of the different vital parameter to the observed variation of rSO₂ and HbT within the study group was determined by partial variances. Each partial variance was obtained by dividing the vital parameter’s mean square sum by the model’s mean square sum. The random-coefficient analyses for rSO₂ and HbT were performed with PROC MIXED from SAS 9.3 (SAS, Cary, NC). The data were weighted by the number of data records per patient so that all patients contributed equally to the model. Per patient, covariates with too little variation (Table 1) were replaced by zero in the data file. The significance level was generally set to *P* < 0.05. Periods of hypothermic circulatory arrest were excluded from the random-coefficient model, which is therefore limited to the perfused state. These periods were analyzed specifically as described later in the text. A first-order autoregressive term was not added

to the model since, at the temporal scale of minutes to hours, HbT or rSO₂ were not assumed to have a major influence from their past values such as height has in repeated growth measurements [5, 7]. The effects of using deep hypothermic arrest and effects of age and body weight were studied by adding them as covariates to the model.

Subgroup Analysis of Circulatory Arrest

During hypothermic circulatory arrest, the cerebral rSO₂ is known to exponentially decay to a nadir that represents the deoxygenated state [1, 2, 6, 12, 13]. Per circulatory arrest, the individual decay curve of rSO₂ was fitted by using PROC NLMIXED from SAS 9.3 using the following equation (Eq. 1) [13]:

$$rSO_2 = \beta_0 - (\beta_1 \times \beta [1 - \exp(-\beta_2 \times t)]) \tag{1}$$

In this equation, rSO₂ is the fitted value after *t* min, β₀ is the initial rSO₂ at the start of the circulatory arrest, β₁ is the available rSO₂ reserve above the nadir, and the nadir is β₀ – β₁. The half-life of the exponential decay is *T*_{1/2} = ln(2)/β₂ = 0.693/β₂ [12]. Across the patients, this half-life *T*_{1/2} was correlated by regression analysis to the cerebral rSO₂ reserve (*P* < 0.05).

Table 1 Minimum variation of vital parameters

Vital parameter	Minimum (SD)
CPP (mm Hg)	1
CVP (mm Hg)	1
T _{rectal} (°C)	1
Hct (%)	1
SaO ₂ (%)	1
(pCO ₂ (mm Hg)	1
pH	0.05

SD standard deviation

Table 2 Diagnoses and procedures

Patient no.	Age	Body weight (kg)	Diagnosis	Surgical procedure	Hypothermia <30 °C (min)	Hypothermic circulatory arrest (min)
1	2 years	12	Ebstein anomaly	Hemi-Fontan	90	–
2	6 years	21	Ventricular septal defect	Closure	–	–
3	4 days	3.6	Transposition of great arteries	Arterial switch	100	4
4	12 days	3.6	Complex heart defect	Norwood I	102	7 and 44
5	9 years	23	Ventricular septal defect	Closure	–	–
6	5 months	4.2	Ventricular septal defect	Closure	–	–
7	9 years	27	Ascending aortic aneurysm	Homograft patch	–	–
8	6 days	3.6	Hypoplastic left heart syndrome	Norwood I	127	30
9	2 years	8.0	Coarctation of aorta	Homograft patch	70	18
10	5 months	4.8	Atrioventricular canal	Closure	16	–

Results

Patients

The diagnoses and surgical procedures of the 10 children are listed in Table 2. Their age ranged from 6 days to 9 years, and body weight ranged from 3.6 to 27 kg. During CPB, hypothermia $<30^{\circ}\text{C}$ was applied in 7 children and hypothermic circulatory arrest in 4 patients. Patient no. 4 with complex heart defect died after surgery from cardiac insufficiency. The other patients were discharged from hospital without neurological sequelae.

Illustrative Case

Figure 1 illustrates the cerebral NIRS during monitoring during CBP surgery. Additional monitoring traces of the vital parameters are provided in the electronic Supplementary Fig. 1.

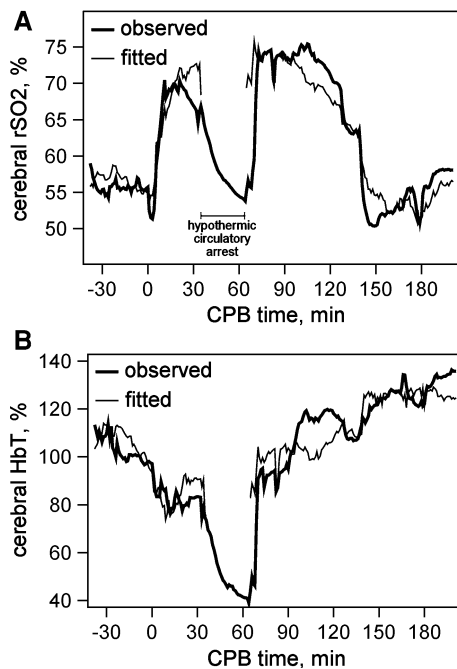


Fig. 1 Monitoring example. Cerebral NIRS monitoring in a 6-day-old girl with hypoplastic left heart syndrome who underwent the Norwood I procedure (patient no. 8). The horizontal X-axis indicate the time lapsed since starting CPB. According to random-coefficient modeling, vital parameters explained $\sim 88\%$ of the $r\text{SO}_2$ variation (a) and 77% of the HbT variation (b). CPB was performed with deep hypothermia lasting approximately 18°C . Hypothermic circulatory arrest was applied between the 33rd and 68th bypass minute. During this period, the cerebral $r\text{SO}_2$ and HbT showed exponential decay without reaching a nadir. In this patient, the lowest $r\text{SO}_2$ occurred shortly after terminating CPB, and further $r\text{SO}_2$ minima occurred at the start of CPB and at the end of the circulatory arrest. Additional monitoring traces of the vital parameters are provided in Supplementary Fig. 1

Study Parameters Before and During CPB

In total, 14,160 data (1,770 1-min records of 8 study parameters in 10 patients) were entered into the analysis. The study parameters at baseline (during -20 to -10 min before CPB) showed some interindividual variation (Table 3). For example, Hct ranged from 26.9 to 50.2%. During CPB, vital parameters generally showed moderate to strong variation except the following: Variation lower than the thresholds listed in Table 1 was observed for T_{rectal} in the 3 nonhypothermia patients, for arterial oxygen saturation in three patients, for pCO_2 in one patient, and for pH in four patients (Supplementary Table 1). Within the total study group, the VIF of the vital parameters ranged between 1.5 and 2.9, indicating no relevant collinearity when using the hierarchical random-coefficient model.

Cerebral $r\text{SO}_2$ Versus Vital Parameters

Cerebral $r\text{SO}_2$ correlated strongly with perfusion pressure and inversely with temperature ($P < 0.05$). These two vital parameters contributed most to the observed $r\text{SO}_2$ variation, whereas the other vital parameters showed only little influence on $r\text{SO}_2$ (Table 4). Overall, 84.7% of the cerebral $r\text{SO}_2$ variation was explained by variations of the vital parameters. The model results were not much different when using temperature-corrected pCO_2 and pH instead of 37°C -adjusted values.

Cerebral HbT Versus Vital Parameters

Cerebral HbT correlated strongly with perfusion pressure, central venous pressure, and temperature and inversely with arterial oxygen saturation ($P < 0.05$). These four vital parameters contributed most to the observed HbT variation,

Table 3 Study parameters at baseline

Parameters	Mean (\pm SD)	Range
Vital parameters at baseline ^a		
MAP (mm Hg)	66.0 (16.2)	50–98
CVP (mm Hg)	9.9 (2.3)	5–12
CPP (mm Hg) ^b	56.1 (16.5)	38–85
Hct (%)	37.7 (6.9)	26.9–50.2
SaO ₂ (%)	96.8 (4.8)	86–100
pCO ₂ (mm Hg) ^c	38.4 (4.2)	31.2–46.5
pH ^c	7.39 (0.04)	7.32–7.45
Cerebral NIRS parameters at baseline ^b		
$r\text{SO}_2$ (%)	60.0 (3.8)	54.9–65.4
HbT ($\mu\text{mol/L}$)	134.3 (27.1)	94–177

^a The baseline is the time period from -20 to -10 min before CPB

^b CPP was determined by $\text{CPP} = \text{MAP} - \text{CVP}$

^c pCO₂ and pH were obtained from arterial blood gas analyses

Table 4 Relation of cerebral NIRS readings to vital parameters

Vital parameters	Random-coefficient model for rSO ₂				Random-coefficient model for HbT ^a			
	Mean regression slope mean (95 % CI)	P ^c	MSq	Partial variance (%) ^d	Mean regression slope mean (95 % CI)	P ^c	MSq	Partial variance (%) ^d
CPP ^a (%)	0.05 (0.02–0.07)	<0.01	107.6	57.3	0.09 (0.02–0.16)	0.016	125.4	19.1
CVP (mm Hg)	0.10 (–0.10 to –0.30)	0.32	7.2	3.8	0.40 (0.01–0.79)	0.044	87.6	13.3
T _{rectal} (°C)	–0.33 (–0.60 to –0.07)	0.014	43.4	23.1	0.84 (0.17–1.51)	0.014	131.0	19.9
Hct (%)	0.05 (–0.18 to 0.27)	0.69	1.1	0.6	0.58 (–0.09 to 1.24)	0.09	62.3	9.5
SaO ₂ (%)	0.05 (–0.13 to 0.24)	0.56	2.4	1.3	–0.45 (–0.73 to –0.17)	<0.01	212.5	32.4
pCO ₂ (mm Hg) ^b	0.08 (–0.05 to 0.21)	0.23	10.2	5.4	0.04 (–0.36 to 0.44)	0.85	0.9	0.1
pH ^b	22.7 (–7.1 to 52.6)	0.14	16.0	8.5	20.2 (–10.0 to 50.4)	0.19	37.2	5.7
Sum			187.9	100			656.9	100
	rSO ₂				HbT ^a			
SD of residuals (%)	2.68 (2.59–2.77)				4.65 (4.49–4.82)			
R	0.92				0.95			
R ² (%)	84.7				90.7			

The relation of the cerebral NIRS parameters rSO₂ and HbT to seven vital parameters was analyzed by a multivariate random-coefficient model that accounts for interindividual differences in the multivariate regression slopes. This table summarizes the pooled estimates of the study group MSq mean square of the rSO₂, HbT changes related to changes in the according vital parameter

- ^a HbT and CPP were expressed as percentage change from the individual baseline, which was the period of –20 to –10 min before CPB
- ^b Significant P values (P < 0.05) are printed in bold. The according regression slopes were significantly different from zero
- ^c The partial variance indicates the contribution of the corresponding vital parameter to the observed variation of rSO₂ (or HbT, respectively) within the study group. Each partial variance was obtained by dividing the corresponding MSq value by the sum of MSq values
- ^d pH and pCO₂ from arterial blood gas analyses determined at 37 °C

whereas the other vital parameters showed only little influence on HbT (Table 4). Overall, 90.7 % of the cerebral HbT variation was explained by variations of the vital parameters. The model results were not much different when using temperature-corrected pCO₂ and pH instead of 37 °C-adjusted values.

Other Covariates

Age, body weight, and deep hypothermic arrest showed no significant effect (P > 0.05) and therefore did not represent a significant source of heterogeneity.

Hypothermic Circulatory Arrest

Five periods of hypothermic circulatory arrest were applied in four patients. With some interindividual differences, the nadir of complete cerebral rSO₂ deployment was estimated as 46.7–52.9 %. Patients no. 3, 8, and 9 started at a relatively high rSO₂ of 64–69 %, with consequently high rSO₂ reserve, and did not reach their estimated nadir during circulatory arrest (Fig. 2). In these three patients, the half-life T_{1/2} of the exponential rSO₂ decay ranged from 5.2 to 9.0 min. Patient no. 4 required two periods of hypothermic circulatory arrest during CPB surgery. Both periods started at a relatively low rSO₂ of 53.6 % with a consequently low

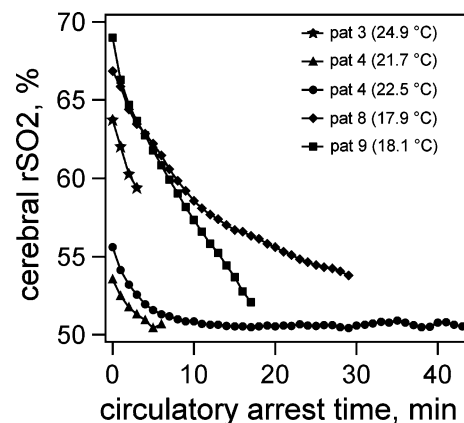


Fig. 2 Cerebral rSO₂ during hypothermic circulatory arrest. The rSO₂ showed an exponential decay during five episodes of hypothermic circulatory arrest in four patients. In a case (closed circles) with a core temperature of 22.5 °C and a relatively low rSO₂ at the start of the circulatory arrest, the nadir was reached after ~15 min. In the other cases, the nadir was not reached because the rSO₂ reserve (the difference between the starting value and the nadir) was sufficiently high and/or the circulatory arrest time was sufficiently short. Among the patients, half-life T_{1/2} of the exponential rSO₂ decay was significantly correlated to rSO₂ reserve (P = 0.016)

oxygen-extraction reserve. In the second period with 44 min’ duration, the nadir was reached after approximately 15 min with no further cerebral rSO₂ deployment during the remaining 29 min. In this patient, half-life T_{1/2}

Table 5 Individual minimum of cerebral rSO₂

Patient no.	Minimum rSO ₂ (%) ^a	CPP (%) ^{b,c}	T _{rectal} (°C) ^c	Hct (%) ^c	Procedural landmark	Duration of rSO ₂ <50 % (min)
1	49.4	26.3	36.0	34	10 min before terminating CPB	1
2	47.4	31.2	36.5	20	14 min after starting CPB	10
3	59.0	62.8	33.1	28	20 min before terminating CPB	–
4	44.5	54.9	36.9	27	77 min after terminating CPB	147
5	47.9	22.7	37.7	19	15 min before terminating CPB	3
6	49.2	28.0	36.3	27	5 min after starting CPB	2
7	52.2	24.8	35.7	19	1 min after starting CPB	–
8	50.3	71.2	33.0	33	10 min after terminating CPB	–
9	52.1	0.0	18.7	25	At end of circulatory arrest	–
10	47.2	55.6	33.5	23	21 min before terminating CPB	25

^a Individual minimum rSO₂ with rSO₂ <50 % printed in bold

^b Central perfusion pressure, given as percentage of its baseline value

^c CPP, T_{rectal}, and Hct at minimum rSO₂

was 1.8 min during the first and 2.1 min during the second circulatory arrest. Rectal temperature was 22–23 °C during this time. Among the patients, half-life $T_{1/2}$ was significantly correlated to the rSO₂ reserve ($P = 0.016$), i.e., the greater the rSO₂ reserve, the longer the time to nadir.

Individual Minimum of Cerebral rSO₂

In six patients, cerebral rSO₂ decreased to <50 % during or after CPB (Table 5). In five patients, this occurred during episodes of arterial hypotension (CPP 26.3–55.6 % of baseline), whereas the patients were normothermic ($T_{\text{rectal}} \geq 36$ °C). One case (patient no. 4) showed a prolonged period of rSO₂ <50 % after CPB, with the minimum rSO₂ being <45 % (Table 5).

Discussion

The current literature contains no studies that closely relate cerebral NIRS to vital parameters. This pilot study evaluated methodologies for monitoring and interpretation of cerebral NIRS readings during cardiovascular bypass surgery in children. Although the number of patients was small, the study showed significant results because of the detailed data (1,770 1-min-records with 14,160 data) and the close relation of the NIRS readings to the vital parameters. Even on an individual basis the NIRS readings could be interpreted in relation to the vital parameters, which is a prerequisite for NIRS-based optimization of the vital parameters.

The patients were enrolled prospectively and consecutively, and thus represented a random sample of pediatric patients who required CPB surgery. This study provides evidence that the relations between cerebral rSO₂ and HbT

can be derived from purely observational and noninvasive NIRS measurements when using a hierarchical random-coefficient model that accounts for unknown but true differences among the patients. The applied spatially resolved NIRS represents advanced technology with its readings being stabilized by using four lasers at different wavelengths and a sensor-coupling compensation. Its measurements are well reproducible specifically in trend monitoring [18]. In experimental studies, its cerebral rSO₂ correlated well to jugular venous oxygen saturation during CPB [2]. Currently cerebral NIRS monitoring is not fully quantitative because the readings may be affected by an offset and slope; however, semiquantitative changes can be well studied. This study focused on such changes in relation to vital parameters. The results indicate that NIRS could be used to assess the overall effect of vital parameter changes on mixed cerebral oxygenation during CPB surgery. Because body temperature, Hct, and other vital parameters are modifiable during CPB, the cerebral NIRS response to optimizing these vital parameters could be monitored and analyzed. The observed relations between NIRS readings and vital parameters are discussed in detail in the following text.

Venous-Weighted Cerebral rSO₂

The venous-weighted cerebral rSO₂ contains information about the brain's oxygen extraction. Detecting extensive cerebral rSO₂ decreases is clinically relevant as has been observed in children undergoing CPB surgery [14]. In this study, perfusion pressure and body temperature were the most relevant determinants of rSO₂. At greater perfusion pressure, cerebral blood flow may increase so that less oxygen must be extracted from the circulating blood, and venous-weighted rSO₂ may increase. This is indicated by

the observed significant positive relation of rSO_2 to CPP (Table 4). At lower body temperature, the cerebral metabolism is decreased and requires less oxygen such that the venous-weighted rSO_2 may increase. This is indicated by the significant inverse relation of rSO_2 – T_{rectal} (Table 4). Considering the additive effects of perfusion pressure and body temperature, the lowest rSO_2 may be expected during normothermic arterial hypotension. Consistent with this, in our study five of six rSO_2 minima $>50\%$ occurred during such episodes (Table 5). This also explains why the pre-bypass and early postbypass periods are vulnerable times for provision of adequate cerebral oxygenation because these periods may be characterized by blood-pressure instability while the brain is not protected by hypothermia [6]. Due to wide confidence intervals, the other model coefficients were not significant. However, their trends were reasonable: In the absence of right-heart failure, greater central venous pressure mostly indicates the presence of more blood volume in the vasculature, which may facilitate cerebral perfusion and thus increase rSO_2 . The presence of more oxygen carriers in the blood at greater Hct may also increase rSO_2 . At greater arterial SaO_2 , hemoglobin both in the arteries and veins will have greater oxygen saturation if other factors of cerebral oxygen metabolism are constant (e.g., oxygen extraction and blood flow), thus increasing rSO_2 . Hypocapnia can cause cerebral vasoconstriction and subsequent hypoxemia with low rSO_2 , e.g., during hyperventilation. Acidosis may occur during low-perfusion states that require increased oxygen extraction from the blood. Apart from some differences regarding the slopes and significance levels of the model coefficients, the observed relations between rSO_2 and the vital parameters were consistent with findings of other studies [2, 8, 10, 19, 22, 24].

NIRS Parameter HbT

Compared with rSO_2 , the NIRS parameter HbT is also of scientific interest, but is not mandatory. HbT is proportional to regional cerebral blood volume and Hct within the tissue underneath the NIRS sensor [19]. The random-effects model accounts for changes in Hct such that the following also refers to the regional cerebral blood volume: In this study, perfusion pressure, central venous pressure, body temperature, and arterial oxygen saturation were major determinants of HbT. At greater perfusion pressure, cerebral blood volume increases as indicated by the significant positive relation of HbT–CPP (Table 4). In the absence of right-heart failure, greater central venous pressure mostly indicates the presence of more blood volume in the vasculature, which may explain the positive relation to HbT. During hypothermia, cerebral oxygen consumption decreases such that the cerebral blood flow may decrease. Because cerebral blood flow and cerebral blood volume are

in general positively correlated, and because HbT is proportional to cerebral blood volume, the observed positive relation of HbT– T_{rectal} can be explained. The significant inverse HbT– SaO_2 relation indicates that an SaO_2 decrease is associated with an HbT increase, i.e., the hypoxemia was a potent cerebral vasodilator (Table 4). Due to wide confidence intervals, the other model coefficients were not significant. However, their trends were reasonable: At greater Hct, hemoglobin content in the cerebral vasculature is greater. Hypercapnia can cause cerebral vasodilatation with subsequently increased cerebral blood volume. Acidosis may occur during hypovolemia with subsequently decreased cerebral blood flow and blood volume. The presented HbT results are novel because most NIRS monitors do not provide HbT readings.

Hypothermic Circulatory Arrest

Hypothermic circulatory arrest represents a specific situation during CPB where the cerebral oxygen supply is stopped. However, even during deep hypothermia, the cerebral oxygen demand persists as indicated by the arterio-venous oxygen saturation difference during active bypass flow. In patients during hypothermic circulatory arrest, this and other studies observed an exponential decay of rSO_2 toward a nadir [1, 2, 6, 12, 13]. This decay may indicate successive oxygen extraction from the locally available HbO_2 , and its half-life $T_{1/2}$ may indicate how well cerebral oxygen metabolism is maintained during the arrest. In three of our patients, half-life $T_{1/2}$ was within the normal values of another study [12], whereas one patient with low rSO_2 reserve consequently had a small half-life $T_{1/2}$ and reached the rSO_2 nadir. Except from observational NIRS research monitoring, this decrease in cerebral oxygen saturation was not evident from any other measure. Jugular bulb oximetry would not have been a solution because it cannot assess cerebral oxygenation when cerebral perfusion is stopped. Other investigators have observed that deep hypothermia of 13–16 °C at onset of circulatory arrest is associated with a much slower rSO_2 decay than hypothermia >20 °C, and this might be studied further [6].

Some other studies have correlated NIRS-based cerebral rSO_2 to procedural landmarks during CPB, such as hypothermic circulatory arrest or rewarming [10, 21]. However, the relation between cerebral NIRS readings and vital parameters during CPB in children has generally not been analyzed at a fine temporal scale. A prerequisite for such analysis is a suitable statistical model that has been applied in this study.

There are some minor limitations to this study. The number of 10 patients was small; however, the number of data (14,160) was large. The study indicates that a small patient number is sufficient for obtaining significant results

such that small-sized subgroups could be compared in future studies. Among such subgroups (for example, neonates vs. older children), the relation between NIRS and vital parameters might differ somewhat. The results of the present study did not intend to investigate such subgroups; however, they provide results that may be generally expected in children during CPB surgery. The applied NIRS monitor was semiquantitative, which was sufficient because the study focused on changes rather than on absolute values. A fixed differential pathlength factor was used, although it may vary interindividually with age or other variables. This was statistically considered by the random effects. The bypass flow rate was not included into the statistical model because otherwise the cardiac output in mL/min before and after CPB should also be included; however, this parameter was unknown. However, the model included the central perfusion pressure that is related to the body's perfusion. A catheter-based jugular venous saturation was not added to the analysis because cerebral rSO_2 was used instead. Arterial blood gas sampling was intermittent with interpolation to 1-min intervals. Sampling at 1-min intervals might have shown closer 95 % confidence intervals for pH and pCO_2 coefficients and thus more significant correlations to rSO_2 and HbT; however, doing so would be impractical. Continuous in-line blood gas monitoring with comparison to intermittent blood gas samples could be a valuable solution for having real-time blood gas results at 1-min intervals [23]. Hct sampling was also intermittent; however, according changes are more predictable because they are predominately related to hemodilution at the start of CPB and to intraoperative transfusions.

In the future, cerebral NIRS monitoring should become more quantitative to facilitate intraindividual follow-up and interindividual comparisons. For this purpose, the hemoglobin-dominated NIRS measurements at 700–900 nm could perhaps be normalized by an additional water-dominated NIRS measurement at the small spectral window around 1,064 nm, where the scattering is approximately 30 % lower than at 700 nm [9, 25]. In addition, time-resolved NIRS could be further developed for differentiating between light scattering and absorption.

In conclusion, NIRS readings of cerebral hemoglobin content and tissue oxygen saturation correlate well to vital parameters during CPB surgery in children. NIRS may therefore become a monitoring device for the neuroprotective optimization of those vital parameters.

References

1. Abdul-Khaliq H, Schubert S, Troitzsch D, Huebler M, Boettcher W, Baur MO et al (2001) Dynamic changes in cerebral oxygenation related to deep hypothermia and circulatory arrest evaluated by near-infrared spectroscopy. *Acta Anaesthesiol Scand* 45:696–701
2. Abdul-Khaliq H, Troitzsch D, Schubert S, Wehsack A, Bottcher W, Gutsch E et al (2002) Cerebral oxygen monitoring during neonatal cardiopulmonary bypass and deep hypothermic circulatory arrest. *Thorac Cardiovasc Surg* 50:77–81
3. Armitage P, Berry G (1994) Statistical methods in medical research, 3rd edn. Blackwell Science, Oxford
4. Ashwood ER, Kost G, Kenny M, Bacher A (1983) Temperature correction of blood-gas and pH measurements. Effects of body temperature on blood gases. *Clin Chem* 29:1877–1885
5. Chatfield C (1989) The analysis of time series: an introduction, 4th edn. Chapman & Hall, London
6. Daubeney PE, Smith DC, Pilkington SN, Lamb RK, Monro JL, Tsang VT et al (1998) Cerebral oxygenation during paediatric cardiac surgery: identification of vulnerable periods using near infrared spectroscopy. *Eur J Cardiothorac Surg* 13:370–377
7. Dobson AJ, Barnett AG (2008) An introduction to generalized linear models, 3rd edn. CRC Press, Boca Raton
8. Ginther R, Sebastian VA, Huang R, Leonard SR, Gorney R, Guleserian KJ et al (2011) Cerebral near-infrared spectroscopy during cardiopulmonary bypass predicts superior vena cava oxygen saturation. *J Thorac Cardiovasc Surg* 142:359–365
9. Hale GM, Querry MR (1973) Optical constants of water in the 200-nm to 200-microm wavelength region. *Appl Opt* 12:555–563
10. Hoffman GM, Stuth EA, Jaquiss RD, Vanderwal PL, Staudt SR, Troshynski TJ et al (2004) Changes in cerebral and somatic oxygenation during stage 1 palliation of hypoplastic left heart syndrome using continuous regional cerebral perfusion. *J Thorac Cardiovasc Surg* 127:223–233
11. Jöbsis FF (1977) Noninvasive infrared monitoring of cerebral and myocardial oxygen sufficiency and circulatory parameters. *Science* 198:1264–1267
12. Kurth CD, Steven JM, Nicolson SC (1995) Cerebral oxygenation during pediatric cardiac surgery using deep hypothermic circulatory arrest. *Anesthesiology* 82:74–82
13. Kussman BD, Wypij D, DiNardo JA, Newburger JW, Mayer JE Jr, del Nido PJ et al (2009) Cerebral oximetry during infant cardiac surgery: evaluation and relationship to early postoperative outcome. *Anesth Analg* 108:1122–1131
14. Kussman BD, Wypij D, Laussen PC, Soul JS, Bellinger DC, DiNardo JA et al (2010) Relationship of intraoperative cerebral oxygen saturation to neurodevelopmental outcome and brain magnetic resonance imaging at 1 year of age in infants undergoing biventricular repair. *Circulation* 122:245–254
15. Littell RC, Milliken GA, Stroup WW, Wolfinger RD, Schabenberger O (2006) SAS for mixed models, 2nd edn. SAS Institute, Cary
16. Menke J (2009) Diagnostic accuracy of contrast-enhanced MR angiography in severe carotid stenosis: meta-analysis with meta-regression of different techniques. *Eur Radiol* 19:2204–2216
17. Menke J (2010) Bivariate random-effects meta-analysis of sensitivity and specificity with SAS PROC GLIMMIX. *Methods Inf Med* 49:54–64
18. Menke J, Voss U, Möller G, Jorch G (2003) Reproducibility of cerebral near infrared spectroscopy in neonates. *Biol Neonate* 83:6–11
19. Menke J, Stöcker H, Sibrowski W (2004) Cerebral oxygenation and hemodynamics during blood donation studied by near-infrared spectroscopy. *Transfusion* 44:414–421
20. Menke J, Larsen J, Kallenberg K (2011) Diagnosing cerebral aneurysms by computed tomographic angiography: meta-analysis. *Ann Neurol* 69:646–654
21. Morimoto Y, Niida Y, Hisano K, Hua Y, Kemmotsu O, Murashita T et al (2003) Changes in cerebral oxygenation in children undergoing surgical repair of ventricular septal defects. *Anaesthesia* 58:77–83

22. Moritz S, Rochon J, Volkel S, Hilker M, Hobbhahn J, Graf BM et al (2010) Determinants of cerebral oximetry in patients undergoing off-pump coronary artery bypass grafting: an observational study. *Eur J Anaesthesiol* 27:542–549
23. Ottens J, Tuble SC, Sanderson AJ, Knight JL, Baker RA (2010) Improving cardiopulmonary bypass: does continuous blood gas monitoring have a role to play? *J Extra Corpor Technol* 42:191–198
24. Tisdall MM, Taylor C, Tachtsidis I, Leung TS, Elwell CE, Smith M (2009) The effect on cerebral tissue oxygenation index of changes in the concentrations of inspired oxygen and end-tidal carbon dioxide in healthy adult volunteers. *Anesth Analg* 109:906–913
25. van Staveren HJ, Moes CJ, van Marie J, Prah SA, van Gemert MJ (1991) Light scattering in Intralipid-10% in the wavelength range of 400–1100 nm. *Anesth Analg* 30:4507–4514
26. Watzman HM, Kurth CD, Montenegro LM, Rome J, Steven JM, Nicolson SC (2000) Arterial and venous contributions to near-infrared cerebral oximetry. *Anesthesiology* 93:947–953
27. Wolf M, Evans P, Bucher HU, Dietz V, Keel M, Strebel R, von Siebenthal K (1997) Measurement of absolute cerebral haemoglobin concentration in adults and neonates. *Adv Exp Med Biol* 428:219–227